# Malignant Tumors of Peripheral Nerves

15

Simon Ching-Shun Kao, David M. Parham, and Christine Fuller

## Definition

Malignant peripheral nerve sheath tumors (MPNST) represent a group of malignant spindle cell sarcomas with evidence of nerve sheath differentiation and/or arising from a peripheral nerve. Tumors showing origin from epineurial connective tissue or vascular structures are not considered to represent MPNST. Older/prior terminology for MPNST includes malignant neurilemmoma, malignant schwannoma, neurofibrosarcoma, and neurogenic sarcoma [1]. A number of histologic subtypes have been described. The majority are high grade aggressive sarcomas that show a strong tendency for local recurrence and metastases despite aggressive therapeutic measures [2].

## Clinical Features and Epidemiology

There is a strong association between MPNST and Neurofibromatosis Type 1 (NF1), with 50 % of all MPNSTs arising within this patient population [3]. Approximately 10 % of individuals with NF1 will develop an MPNST over their lifetime, most of these tumors representing malignant degeneration occurring within preexisting plexiform neurofibromas. One study of 476 NF1 patients documented a strong association between the presence of subcutaneous neurofibromas and internal plexiform neurofibromas, with an even stronger correlation between the presence of internal plexiform neurofibromas and MPNST [4]. The remainder of MPNSTs will arise de novo, approximately 5–10 % representing radiation-induced sarcomas [1]. There is no particular gender predilection, and MPNSTs have been documented throughout a wide age range including children and the elderly. The majority however tend to present in adults with a median age in the mid 40s [5]. MPNSTs arising in the NF1 population tend to present up to a decade earlier, and these patients' tumors also tend to be larger [3, 6].

The majority of MPNST arise from larger peripheral nerves or within deep soft tissues, the most frequent sites including brachial plexus, sciatic, and paraspinal nerves, proximal upper and lower extremities, and buttock regions [5]. They have also been documented in a wide variety of locations throughout the body. Well over 50 cases of spinal MPNST have been reported [7–13]. No particular spinal level is preferentially involved, and interestingly a significant proportion of spinal MPNST exhibit rhabdomyoblastic elements (Malignant Triton Tumor; see histologic description below) [14–17]. MPNST represents one of the most aggressive tumors that may involve structures of the head and neck region [6]. It may arise from cranial nerves, particularly the vestibular [18], vagus [18], facial [18, 19], and trigeminal [19, 20]. Other sites include not only brachial plexus [21], but also scalp and bony structures (base of skull [22–25], sinuses [26, 27], and bones of the jaw) [28, 29], as well as the parotid gland [30–32]. Case reports/small case series document cutaneous MPNSTs [33–35], a proportion of which apparently arose from underlying neurofibromas. Primary cardiac [36], hepatic [37], bile duct [38], colonic [39], uterine [40–42], breast [43, 44], renal [45], and intraosseous [46] MPNST have all been described. Though plexiform neurofibroma is by far the most frequent precursor lesion, MPNSTs have been found rarely arising from

S.C.-S. Kao, MBBS, DMRD, DABR (✉)
Department of Radiology, University of Iowa Healthcare, 200, Hawkins Drive, Iowa City, IA, USA
e-mail: simon-kao@uiowa.edu

D.M. Parham, M.D.
Department of Pathology and Laboratory Medicine, Children's Hospital Los Angeles/University of Southern California, 4650 Sunset Blvd., #43, Los Angeles, CA 90027, USA
e-mail: daparham@chla.usc.edu

C. Fuller, M.D.
Department of Pathology, Virginia Commonwealth University Health System, 1101 East Marshall St, PO Box 980662, Richmond, VA, USA
e-mail: cfuller@mcvh-vcu.edu

D.M. Parham et al. (eds.), *Pediatric Malignancies: Pathology and Imaging*,
DOI 10.1007/978-1-4939-1729-7_15, © Springer Science+Business Media New York 2015

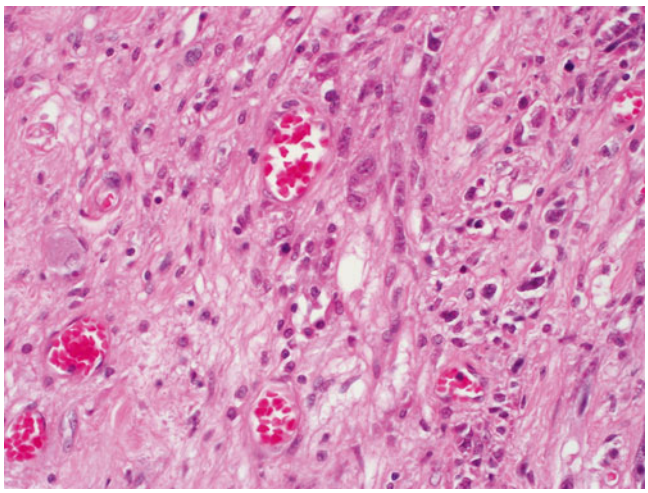

**Fig. 15.1** MPSNT arising from ganglioneuroma. A ganglionic tumor with low grade schwannoma cell stroma segues into a high grade spindle cell neoplasm, X400

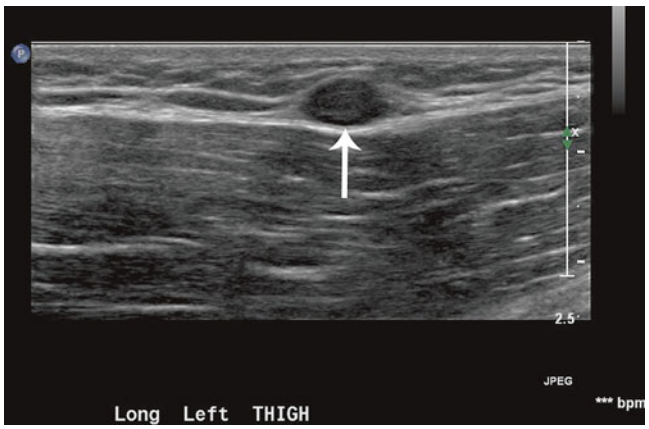


**Fig. 15.2** Neurofibroma of left thigh in an 18-year-old boy. Longitudinal view of the thigh shows a focal hypoechoic mass (*arrow*) in the deep subcutaneous plane against the echogenic muscle fascia with homogeneous echotexture. Excision biopsy showed neurofibroma

ganglioneuroma (Fig. 15.1) [47], hybrid schwannoma/perineurioma [48], or schwannoma [18].

Patients with MPNST tend to be symptomatic, presenting with an enlarging mass, sometimes associated with neurologic symptoms (pain, sensory deficits, and weakness), dependent upon the underlying nerve involved. A rapidly enlarging mass that is mobile perpendicular to the course of a peripheral nerve or that yields a Tinel's sign on percussion is highly suspect for MPNST [1]. Likewise any enlarging mass detected within a patient with NF1 should be considered MPNST until proven otherwise.

## Imaging Features

### Imaging Features of Malignant Peripheral Nerve Sheath Tumors (MPNSTs)

Before describing the imaging features of MPNST, benign PNSTs (neurofibroma and schwannoma) are briefly discussed. Distinguishing imaging features of malignant versus benign tumors are emphasized.

### Neurofibroma

Neurofibroma is a non-encapsulated benign peripheral nerve sheath tumor that has been described in three forms: localized, diffuse, and plexiform [49, 50]. Approximately 90 % are of the localized variety; most are superficial affecting cutis and sub-cutis. The diffuse form is uncommon, primarily affecting children and young adults, involving the subcutaneous tissues of the head and neck region, trunk, and extremity, showing a plaque-like elevation of the skin and thickening of the sub-cutis and may extend to the fascia over muscle [51]. The majority of both localized and diffuse forms is not associated with neurofibromatosis type 1 (NF-1), also known as von Recklinghausen's disease. However in the setting of NF-1, the neurofibromas tend to be larger, multiple, and deep in location. The plexiform form of neurofibroma is pathognomonic of NF-1, presenting usually in early childhood as a tortuous mass involving a long segment of a major nerve trunk and expanding into the nerve branches. It may be superficial or deep in location, exhibiting different MR imaging characteristics (see below). Fifty percent of plexiform neurofibromas occur in the head and neck, face, and larynx.

#### Plain Film Radiography

Plain radiography may show enlargement of neuroforamen when a dumb-bell shaped neurofibroma is involving a spinal nerve root.

#### Ultrasonography

High-resolution sonography of a neurofibroma shows a round homogeneous hypoechoic mass (Fig. 15.2) located centrally along the course of a peripheral nerve with distal acoustic enhancement, simulating a cystic lesion (pseudocystic appearance) [52, 53]. A sonographic target lesion with hypoechoic periphery and hyperchoic center may be seen, corresponding to myxomatous peripheral and fibrocollagenous central regions, respectively [53]. In diffuse neurofibromas, hyperechoic masses permeated by multiple interconnecting hypoechoic tubular or nodular structures have been reported in the subcutaneous fat zone. Differential diagnoses include cutaneous lymphoma, angiomatous lesions, cellulitis, and hemorrhage [54]. Sonography, even with duplex and color Doppler techniques, is not able to distinguish among neurofibromas, schwannomas, and malignant peripheral nerve sheath tumors [53, 55].

**Fig. 15.3** Diffuse neurofibromas in a 14-year-old girl with neurofibromatosis type 1. Contrast-enhanced axial CT image of the pelvis shows a network of interconnecting soft tissues masses in both gluteal subcutaneous fat due to multiple neurofibromas

### Computed Tomography

On CT, *localized* neurofibromas appear as a well-defined hypodense (compared with muscles) mass from the presence of Schwann cells (fat content of myelin), myxoid tissue (high water content), entrapment of fat, and cystic areas of hemorrhage or necrosis [56]. After intravenous contrast injection, over half of neurofibromas show little or no contrast enhancement (Fig. 15.3). Visible bony erosions associated with dumbbell tumors are seen with CT [57].

### Magnetic Resonance Imaging

On MRI, a neurofibroma is spindle or ovoid in shape and is in contiguity with a specific nerve [58]. It shows low to intermediate signal intensity (or isointense to adjacent muscles) on T1W images and high signal intensity on T2W images. The high signal intensity on T2W images may be homogeneous or showing a characteristic "target sign" with a hyperintense periphery and a hypointense central region [59–61]. The high peripheral signal is related to myxoid and water contents and the central low signal is related to dense collagen and fibrillary tissues. It is important to use a wide window setting to allow demonstration of this sign [62]. After intravenous contrast, enhancement is inhomogeneous in two-thirds of cases and uniform in the rest. A neurofibroma is typically fusiform in shape with tapering ends contiguous with the parent nerve. When large, the tumor has a fascicular appearance (fascicular sign). A "split-fat" sign has been described when a neurofibroma originating from the nerve in an intramuscular location is surrounded by a rim of fat. Muscle atrophy may be seen in the muscle supplied by the nerve with neurofibroma. The *diffuse* form of neurofibroma presents as an ill-defined network of interconnecting neurofibromas extending through the involved subcutaneous tissue, showing low signal intensity on T1W images, high signal intensity on T2W images, and significant intravenous contrast enhancement on MR imaging. Prominent internal vascularity is common [51]. *Plexiform* neurofibromas, when deep, appear as hypodense multilobular masses within a major nerve distribution on CT scans and large conglomerate of masses of neurofibromas on MR imaging (Fig. 15.4). When superficial, plexiform neurofibromas in patients with NF-1 tend to be unilateral, have nontarget signal characteristics, exhibit a diffuse and infiltrative morphology, extend to the skin surface in a branching reticular fashion with small fascicles or nodules (Fig. 15.5), and can be mistaken for venous malformation by MR imaging [63–65].

**Fig. 15.4** Deep plexiform neurofibromas in a 17-year-old boy. Coronal HASTE MRI imaging of the abdomen and pelvis shows a large conglomerate of masses in the right psoas muscle, most showing "target sign". Partial excisional biopsy of some of these masses shows "neurofibroma without evidence of malignant change"

## Schwannoma (Neurilemmoma)

Schwannoma is an encapsulated (within the epineurium) nerve sheath tumor presenting as a slowly growing soft tissue mass involving nerve trunks in limbs, head and neck, posterior mediastinum, and retroperitoneum [49, 66]. The mass is usually painless unless large enough to compress the adjacent nerve. Those associated with NF-1 are usually multiple or plexiform. Schwannomas associated with neurofibromatosis type 2 (NF-2) tend to be central in location [57]. Larger lesions may undergo cystic degenerative changes, hemorrhage, calcification, and fibrosis.

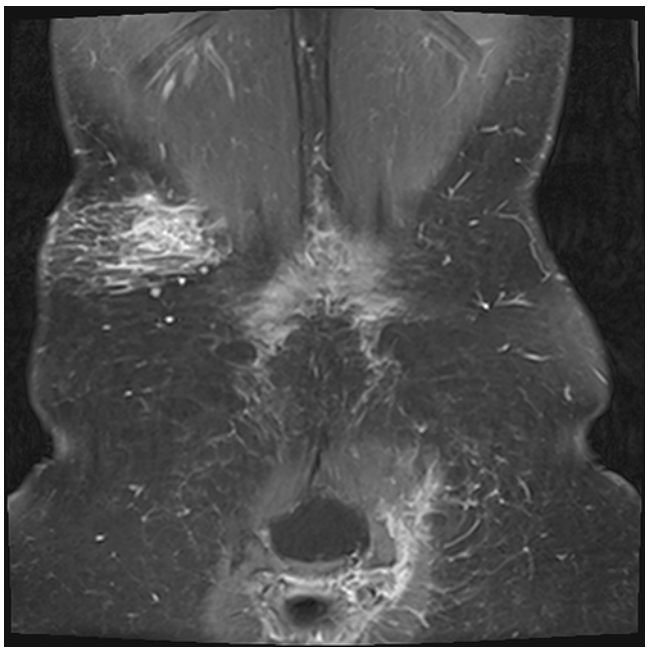

**Fig. 15.5** Superficial plexiform neurofibromas in a 19-year-old female with neurofibromatosis type 1. Post-contrast coronal fat-saturated T1W MRI shows a diffuse infiltrative and reticular branching pattern of plexiform neurofibromas in the *right* flank and *left* gluteal regions

### Plain Film Radiography

Plain radiography usually does not reveal the mass itself, but may show scalloping of bone adjacent to the tumor.

### Ultrasonography

Ultrasonography may show, especially in large nerves, a mass eccentrically positioned with respect to the affected nerve. However, there may be limitations, even with meticulous scanning technique, in demonstrating this eccentric positioning in up to 40 % [55].

### Computed Tomography

On CT scan, schwannoma appears as a well-defined isodense or hypodense mass compared to muscles and shows enhancement after IV enhancement except in necrotic areas. Scalloping of the adjacent bone and expansion of the spinal canal are characteristic features on CT (Fig. 15.6a, b).

### Magnetic Resonance Imaging

MR imaging findings are similar to those described in neurofibromas, including a mass with a fusiform, spindle, or oval shape, in contiguity with a specific nerve, and showing a target sign, and "split-fat" sign. A mass eccentrically positioned in relation to the nerve and showing heterogeneity with cystic degenerative changes suggests a schwannoma [67]. A low signal peripheral rim (epineurium) is seen in 70 % of schwannomas versus in 30 % of neurofibromas [68–70]. The target sign in schwannoma is attributed to a central area of more cellular Antoni type A neurilemmoma and to a peripheral rim of hypocellular Antoni type B neurilemmoma [71].

## Malignant Peripheral Nerve Sheath Tumor (MPNST)

Malignant peripheral nerve sheath tumor is a spindle cell sarcoma arising from a peripheral nerve or its attendant sheath or from a benign PNST [50]. It does not include tumor arising from the epineurium or the vasculature of the peripheral nerves [72]. Typically MPNSTs arise from preexisting plexiform neurofibromas. However it has been documented that 36 % of 34 MPNSTs from a cohort of 1475 NF-1 patients developed MPNSTs without a history of plexiform neurofibromas [73]. While 30-50 % of MPNST are associated with NF-1, only approximately 2–5 % of NF-1 patients develop MPNST [49, 67, 74–76]. Most tumors arise from nodular plexiform tumors

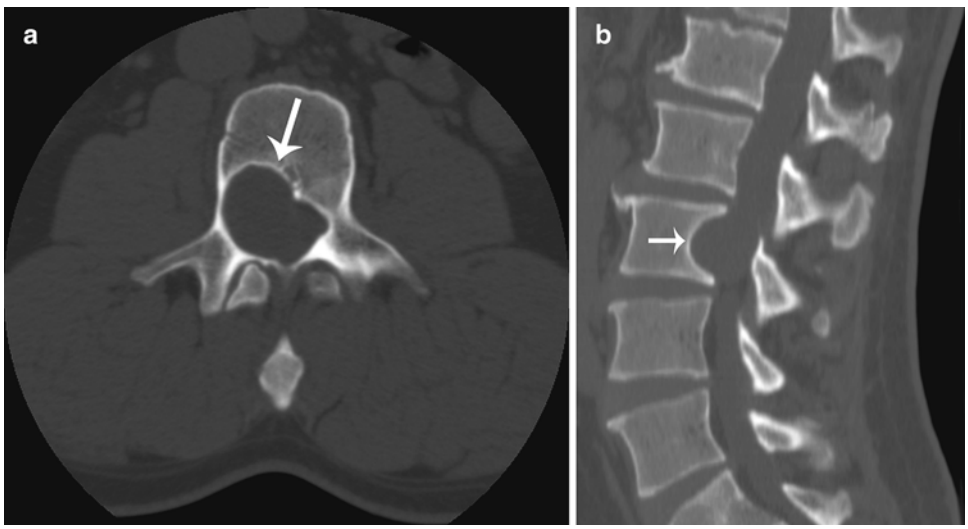


**Fig. 15.6** Intraspinal schwannoma in a 33-year-old adult male with neurofibromatosis type 1. Axial (**a**) and sagittal (**b**) CT images of the lumbar spine show scalloping of the posterior right vertebral margin (*arrows*) at L3 level and expansion of the spinal canal


**Fig. 15.7** Neurofibromatosis type 1 with neurofibroma progression to metastatic malignant peripheral nerve sheath tumor (MPNST). (**a**) Lateral plain radiograph of the thigh shows a soft tissue mass at distal posterior thigh. MRI of the thigh shows a large spindle-shaped posterior thigh mass with (**b**) inhomogeneous high signal intensities on fat-saturated T2W image, (**c**) inhomogeneous low signal intensities and "split-fat" sign (*arrows*) on T1W image, and (**d**) inhomogeneous enhancement on post-contrast fat-saturated T1W image. Biopsy of the mass showed a poorly differentiated MPNST arising within a neurofibroma. (**e**) Axial CT image shows multiple lung metastases

associated within major nerve trunks (such as brachial plexus sacral plexus, and sciatic nerve) and patients tend to be symptomatic presenting with pain, sensory deficits, and weakness. MPNSTs metastasize to the lung, liver, brain, regional lymph nodes, bone and soft tissues, skin, and retroperitoneum, and carry a poor prognosis [76].

## Plain Film Radiography

Although often normal, plain radiography may show a soft tissue mass (Fig. 15.7a), secondary changes in adjacent bones (erosion or overgrowth), and is essential for evaluation of metastases to chest (lungs and pleura). Calcification (chondroid, osteoid, or amorphous) is uncommonly seen.

### Ultrasonography

Sonography shows inhomogeneous hypoechoic masses that may have areas of hemorrhage, necrosis and calcifications [50]. A sonographic target sign is not present [53]. Duplex Doppler sonography shows a hypervascular pattern with corkscrew neovasculature, high velocities, and variable spectral waveforms [77].

### Computed Tomography

Multi-detector CT (MDCT) may show abdominal primary tumor and metastases to the abdomen. On CT, MPNSTs are hypodense and ill-defined in outline with marginal enhancement after IV contrast medium.

### Angiography

Angiography may show increased vascularity with characteristic corkscrew vessels at both ends of the tumor due to hypertrophy of the nutrient blood supplies to the nerve [71].

### Magnetic Resonance Imaging

MPNSTs share MR imaging findings described above with benign peripheral neurogenic tumors. The involvement of the entering and exiting nerves results in the spindle shape of most MPNSTs . Although MRI can determine the site, extent, and change in size of plexiform neurofibromas, it does not reliably determine malignant changes [76, 78–80]. While any neurofibroma that rapidly increases in size in patients with NF-1 should be viewed with suspicion for malignant transformation, the growth rate of plexiform neurofibromas that give rise to MPNSTs is not a reliable predictor of malignancy. There may be periods of rapid growth, especially in adolescence, followed by periods of relative inactivity [81, 82]. Features that are concerning for malignancy include: tumor size over 5 cm in diameter, ill-defined margin, heterogeneity, intratumoral cystic changes, fat plane invasion or infiltration, absence of target or fascicular sign [59, 61, 62, 83], peritumoral edema, presence of peripheral enhancement, and history of having MPNST or previous radiation therapy (Figs. 15.7b–d, 15.8a–d). Only evidence of metastases (such as lung, pleura, bone, retroperitoneal node, and bone) is definitive for diagnosis of MPNSTs (Fig. 15.7e). While the split fat sign was present in 76.5 % of benign and larger PNSTs, only 33.3 % of MPNSTs showed this sign [58]. Whole body (head to feet) MRI with several table movement steps has been used in assessing the benign tumor burden in patients in NF-1 [84].

### Nuclear Medicine Imaging

Bone scintigraphy may show findings indicating increased vascularity or mineralization and identify sites of bony metastases.

FDG-PET has recently proven to be useful in detecting metastatic and recurrent disease [85] and in the differentiation between benign and malignant peripheral nerve tumors using qualitative and semiquantitative $SUV_{max}$ (maximum standardized uptake value) assessment [86, 87] (Fig. 15.8e–g). In patients with NF-1, FDG-PET is 95 % sensitive in the detection of MPNSTs. Because of the overlap in $SUV_{max}$ for benign (ranging from 0 to 5.3, mean $1.5 \pm 0.37$) and malignant (ranging from 3.8 to 13.0, mean $8.5 \pm 0.63$) lesions, the addition of PET using 11C-methionine (measuring amino acid transport rate, protein synthesis, and cell proliferation in malignant tissues) has been found to improve specificity from 72 to 91 %[86]. In another series [87], no MPNSTs were detected with an $SUV_{max}$ <2.5 and a small number of benign tumors had an $SUV_{max}$ >3.5. Both benign and malignant peripheral nerve tumors had $SUV_{max}$ between 2.5 and 3.5. The authors recommend that symptomatic neurofibromas with $SUV_{max} \geq 3.5$ should be excised, and lesions with $SUV_{max}$ between 2.5 and 3.5 should be reviewed clinically. In another study, Son and colleagues found varying degrees of FDG uptake in a patient with multiple benign neurofibromas on PET-CT and concluded that a low $SUV_{max}$ may indicate benignity, but a high $SUV_{max}$ does not always indicate malignancy [88]. Using ROC analysis, Warbey et al. found a significant difference in $SUV_{max}$ between early (90 min) and delayed (4 h) imaging and between tumor grades, and recommended using a cutoff $SUV_{max}$ value of 3.5 on delayed imaging to achieve maximal sensitivity in diagnosing MPNST [89]. The overlap of $SUV_{max}$ between different tumor grades, however, did not allow accurate prediction of grade on an individual basis. The authors suggest that tumors with an $SUV_{max}$ in the 3.0–3.5 range should be clinically reviewed at multidisciplinary and multi-specialist management meetings. In another ROC analysis [90], using $SUV_{max}$ thresholds of 4.5, 6.1, and 8.5 were associated with sensitivities of 100, 94, and 65 % and specificities of 83, 91, and 100 %, respectively, for detecting malignancy. The authors also found that benign schwannomas are less reliably distinguished from the MPNSTs based on the $SUV_{max}$. In a pediatric series of NF-1 and plexiform neurofibromas, Tsai found that the $SUV_{max}$ of typical and atypical plexiform neurofibromas (2.49 [SD = 1.50]) was significantly different from MPNSTs (7.63 [SD = 2.96]). Using an $SUV_{max}$ cutoff value of 4.0, sensitivity and specificity were 100 and 94 %, respectively for distinguishing plexiform neurofibromas and MPNSTs [91]. Nodular target lesions seen on MRI in patient with NF-1 and plexiform neurofibromas were found to have increased FDG uptake similar to that of MPNSTs, although they might be benign on biopsy [92]. Careful longitudinal clinical and imaging monitoring were recommended using MRI and FDG-PET to identify lesions of greatest concern to be biopsied. FDG-PET imaging can help in guiding targeted needle core biopsy of PNSTs [90], directing biopsy to the more metabolically active areas of the tumor. A newer tracer with 18 F-thymidine, which detects DNA turnover, may be useful in distinguishing low grade MPNSTs from active benign plexiform neurofibromas [76].

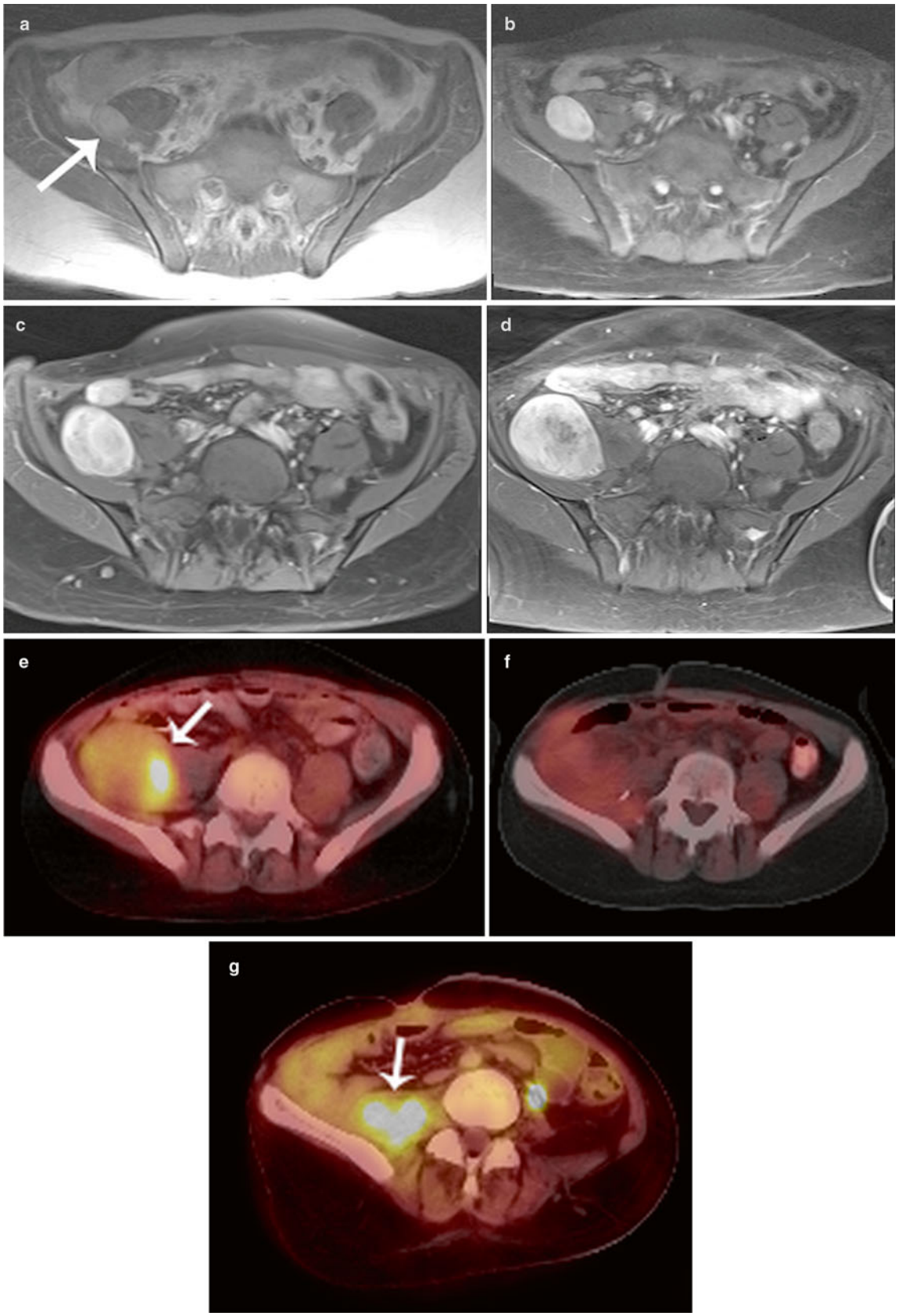


**Fig. 15.8** Progression of neurofibromatosis type 1 first diagnosed in a 14-year-old girl over 5 years into a MPNST. Note progressive increase in size and inhomogeneity of enhancement of a right iliac fossa mass (*arrow*) from (**a**) 2005 (**b**) 2007 (**c**), 2009 and (**d**) 2010. $^{18}$FDG-PET-CT scan in 2010 (**e**) shows a 4.5×6.7 cm mass with SUV $_{max}$ of 5.5 (*arrow*). Excisional biopsy revealed MPNST arising in neurofibroma. (**f**) Follow up $^{18FDG\text{-}PET\text{-}CT}$ scan in 2011 shows no residual tumor (SUV $_{max,}$ 2.0). (**g**) Subsequent follow up in 2012 showed recurrent biopsy-proved MPNST with SUV$_{max}$ of 5.6 (*arrow*)

## Pathology

### Gross and Microscopic Features

#### MPNST

The macroscopic appearance of MPNSTs is highly variable, ranging from large and ominous to subtle. Most will present similar to other soft tissue sarcomas as bulky fusiform or expansive tumors with variable infiltration into surrounding structures. They tend to be large tumors, averaging 6–10 cm in dimension, the majority >5 cm [2, 6]. Identifiable origination from a nerve may or may not be present. MPNSTs have a firm tan to grey interior with areas of hemorrhage and necrosis, similar to other aggressive sarcomas. A pseudocapsule typically represents tumor-infiltrated soft tissue, often with reactive features. At the other end of the spectrum, foci of MPNST arising within an underlying plexiform neurofibroma (malignant degeneration) may not be grossly visible at all, identifiable only at the microscopic level.

Classic / conventional MPNST may display a wide variety of architectural arrangements, frequently posing a significant diagnostic challenge given its resemblance to a number of other soft tissue tumors. The most frequent appearance is one of a hypercellular sarcoma with interwoven fascicles of spindle cells (Fig. 15.9) [93]. Other patterns include a fibrosarcoma-like herringbone pattern, hemangiopericytoma-like with staghorn vasculature, and alternating loose and dense cellular regions (similar to Antoni A and Antoni B regions in schwannomas) (Fig. 15.10) [2]. Perivascular condensation of tumor cells is another helpful feature [2]. Growth within nerve fascicles is also common, though invasion into surrounding tissues is typical. Individual tumor cells are spindle shaped with variable amounts of surrounding pink cytoplasm; nuclei tend to be wavy or indented with tapered ends [2]. Large zones of geographic necrosis are seen in over one half (Fig. 15.11), and mitotic figures are generally easy to find (Fig. 15.12), often numbering several per single high power field.

Fine needle aspiration cytology is being increasing employed in the diagnostic workup of soft tissue lesions, and our knowledge of the salient cytologic features of MPNST has become increasing refined over the past decade. Cytology aspirate smears of MPNST are typically hypercellular with a combination of cohesive cell clusters of variable size and cellularity together with numerous single tumor cells and naked nuclei [94, 95]. A fascicular pattern may be encountered in some cell clusters, though is not universally present; storiform or whorled patterns may also be encountered [30]. A fibrillary background may be present [95]. Individual tumor cells are spindle shaped with variable contour; they may be elongated with tapered ends, kinked, angulated, or comma-shaped [30, 94, 95]. Wavy nuclei, representing a

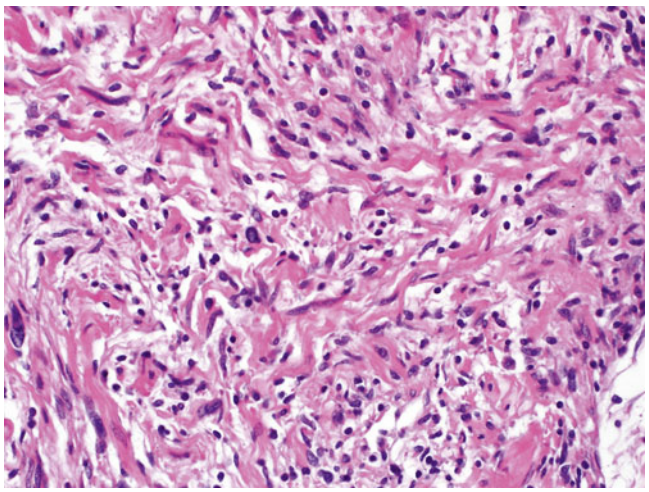

**Fig. 15.9** MPNST, containing spindle cells arranged in interlacing bundles and containing tumor cells with hyperchromatic, enlarged nuclei and wavy contours, X400

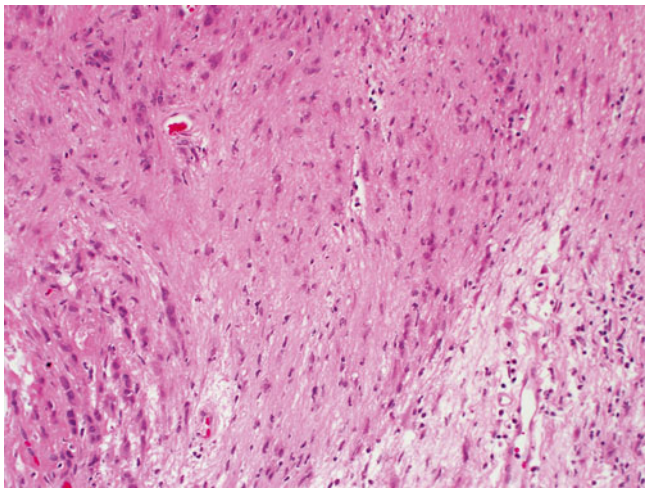

**Fig. 15.10** MPNST with contrasting hypercellular and hypocellular zones, analogous to schwannoma, X200

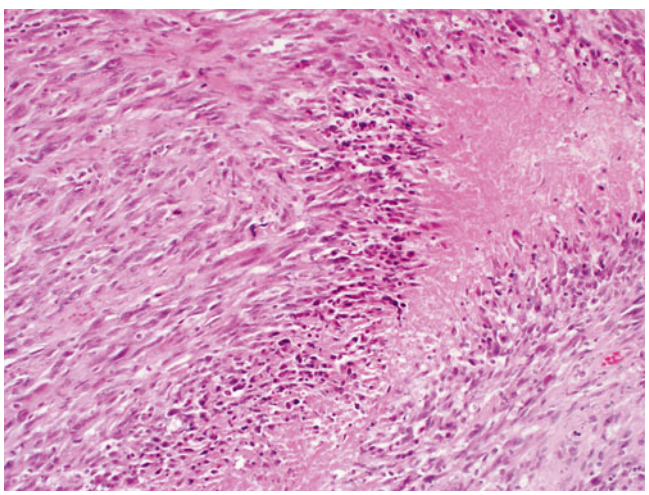

**Fig. 15.11** MPNST with areas of geographic necrosis, X200

quite helpful diagnostic feature when detected, are inconsistently present in MPNST cytology samples [94, 95]. Nuclear pleomorphism is a frequent finding, as are mitotic figures (including atypical forms) [30, 95]. A "dirty" necrotic background material may be seen [30].

The majority (85 %) of MPNSTs are high grade sarcomas. As such, they show evidence of hypercellularity, invasion of surrounding tissues (often with vascular invasion), together with nuclear pleomorphism, elevated mitoses (generally >5 mitoses per 10 high power field), ± necrosis [1]. It is the presence of necrosis that distinguishes high grade from intermediate grade tumors. Low grade MPNSTs make up the minority, appearing histologically similar to cellular neurofibroma, though having comparably increased cellularity and significant nuclear atypia (hyperchromasia and larger nuclear size) (Fig. 15.13a, b).

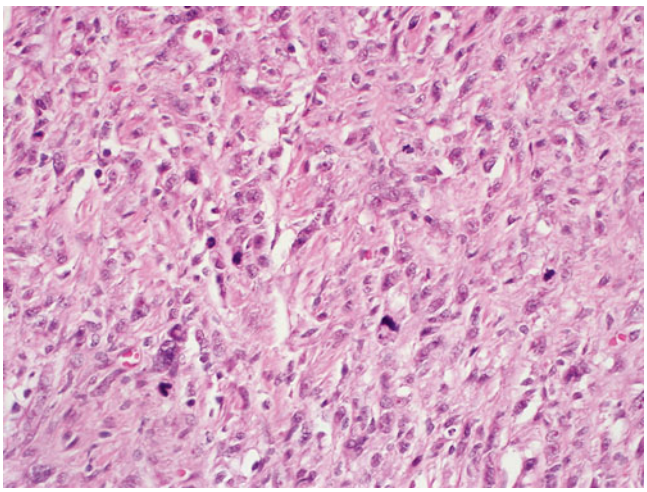

**Fig. 15.12** MPNST with pronounced mitotic activity, X400

Similar to low grade peripheral nerve sheath tumors, MPNSTs may show S100 positivity by immunohistochemistry; unfortunately S100 is detected in only 50 % of cases, and more often only scattered individual cells are S100 positive [18, 96–99]. Low grade MPNSTs tend to have more diffuse S100 positivity compared to their higher grade counterparts [98]. SOX10, a pan-schwannian marker, will be positive in up to 50 % of MPNST, but unfortunately nearly half of MPNSTs will be negative for both SOX10 and S100 [97, 100]. Interestingly, it has been demonstrated that MPNSTs have a heterogeneous cell composition, containing EMA and Glut1-positive perineurial cells, as well as CD34 positive endoneurial fibroblasts [99]. In some cases, cellular structures resembling tactoid bodies can be found (Fig. 15.14). Collagen IV is often present between individual tumor cells or cell groups, positivity tends to be focal and discontinuous [18]. Nestin, GFAP, Leu7, and NSE are demonstrable in some cases [96, 101]. A variety of cell cycle regulatory proteins may also be detected by immunohistochemistry, with low and high grade tumors showing different profiles. Whereas p16 and p27 tend to be positive in low grade MPNSTs, p16 and p27 expression tends to be lost in high grade MPNST, which instead often shows nuclear p53 expression [98, 102, 103].

## MPNST Variants

Approximately 15 % of MPNSTs exhibit some form of divergent differentiation, harboring various mesenchymal or epithelial / epithelioid components [104]. Features of the most well-recognized of these variants are summarized below. It should be noted however, that a wide variety of heterologous elements may much more rarely be encountered; these include areas of fibroblastic [105] smooth muscle differentiation [93],

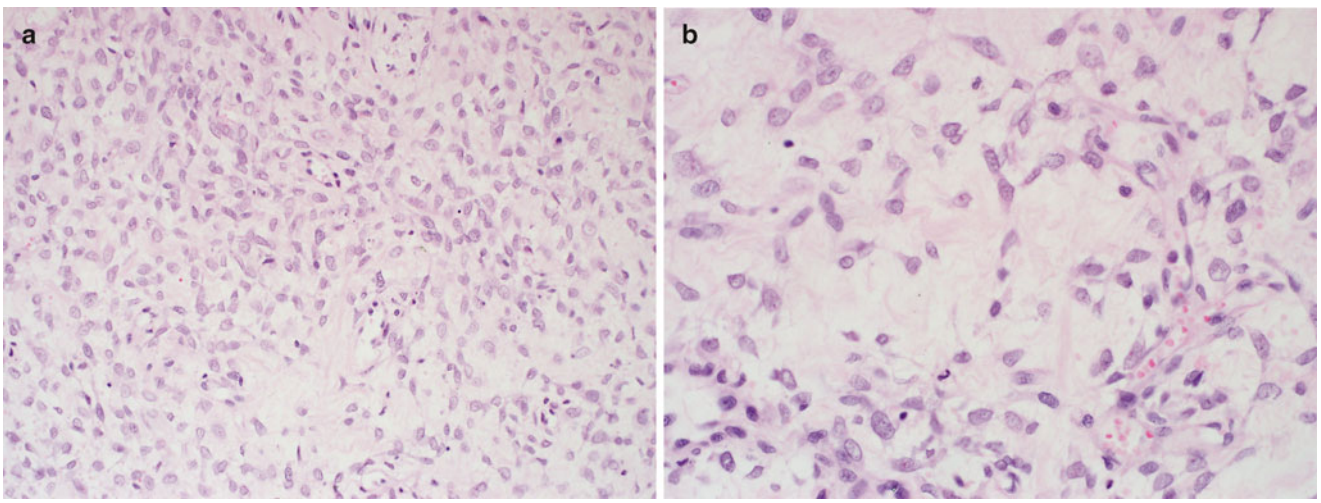


**Fig. 15.13** Low grade MPNST containing hypercellular foci (**a**) amid zones of paucicellular neurofibromatous foci (**b**), X400. The latter exhibits cells with increased size and mild pleomorphism

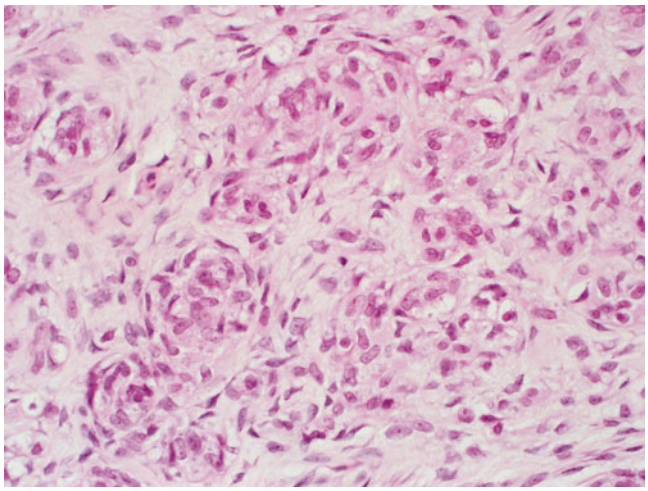

**Fig. 15.14** MPNST with rounded, cellular structures resembling tactoid bodies, X400

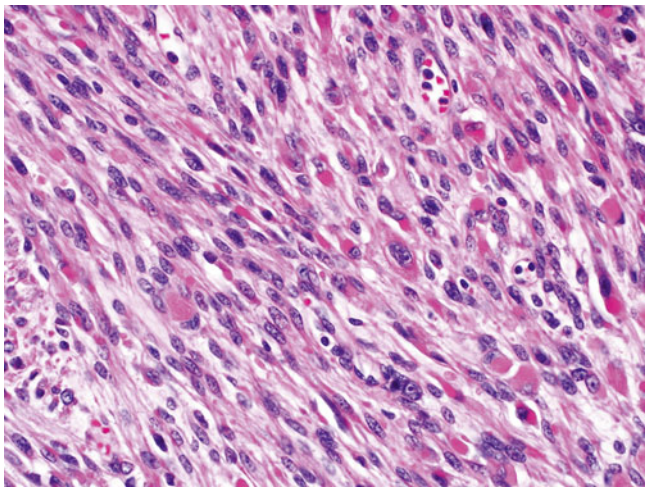

**Fig. 15.15** Malignant triton tumor. The lesion consists of both neural and myogenous elements, the latter exhibiting abundant, eosinophilic cytoplasm and rounded contours, X400

or primitive neuroectodermal tumor (PNET)-like differentiation [106]. Examples of MPNST with pluridirectional differentiation have been described, bearing a mixture of two or more of the following malignant tissue types: epithelioid, rhabdomyoblastic, osteogenic, chondroblastic, lipogenic, and pigmented neuroectoderm [2, 18, 107–111].

## Malignant Triton Tumor (MTT)

MPNST containing a rhabdomyosarcomatous component is termed *malignant triton tumor* (MTT); this represents by far the most frequent form of divergent mesenchymal differentiation within MPNST [16]. Some authors have found that MTT tends to occur in an older population then conventional MPNST (mean age in 5th decade for the former) [112], though others have not found this to be the case [113]. The majority of MTT arise within the context of NF1, they tend to be larger than conventional MPNST, and are more frequent in the head and neck region [112, 113]. Microscopically, the rhabdomyosarcomatous component is typified by rhabdomyoblasts with rounded eosinophilic cytoplasmic bellies, though more elongated cells with discernible cross-striations may be seen (Fig. 15.15) [114]. Immunohistochemical stains for desmin, myoD1, muscle specific actin (MSA), and myogenin are positive in this component [114]. Pluridirectional differentiation is present in a proportion of cases. Similar to conventional MPNST, the vast majority of MTT are high grade aggressive neoplasms.

## Epithelioid MPNST

As the name implies, epithelioid MPNSTs contain variable proportions of cells with an epithelioid appearance. They tend to arise in either superficial or deep soft tissues of the extremities, often involving major nerves [2, 115, 116], though alternate sites have been documented as case reports [42, 117]. There is no association with NF1. In one instance, epithelioid MPNST was documented in the context of a precursor schwannoma, arising in a patient with schwannomatosis and germline SMARCB1 (Ini1) mutation [118]. Microscopically, these lesions have a nodular architecture, composed of cords and rows of rounded epithelioid cells with prominent nucleoli and brisk mitotic activity. They are diffusely positive for S100 and NSE by immunohistochemistry, while they lack more specific melanoma markers. Cytokeratin may be positive in some cases. Similar to other MPNSTs, collagen IV is frequently demonstrable between individual tumor cells and cell groups, corresponding to basement membrane material by electron microscopy [115, 116].

Epithelioid MPNST is not to be confused with *glandular MPNST*, a rare variant which in contradistinction contains well-formed glandular elements resembling benign intestinal-type epithelium. Similar to MTT, three quarters of these patients have underlying NF1, and pluridirectional differentiation is found in a significant proportion of these tumors [119]. In additional to markers typically positive in conventional MPNST, the glandular component is immunopositive for cytokeratin and CEA; chromogranin-positive neuroendocrine differentiation is often present [93, 119].

## Perineurial MPNST (Malignant Perineurioma)

Less than 5 % of all MPNST will show evidence of perineurial differentiation, represented microscopically as a sarcoma containing spindle cells with elongated processes and a whorled to storiform architecture akin to that of benign perineuriomas. Similar to epithelioid MPNST, these tumors are

not associated with NF1, nor do they appear to arise from neurofibromas [120]. They tend to present as large tumors involving the soft tissues of the extremities or trunk; nerve involvement is infrequent. In contrast to conventional MPNST, malignant perineurioma is negative for S100 but positive for EMA, vimentin, glut-1, and claudin-1 [99, 120, 121]. A small proportion will be positive for CD57 and/or CD34. Prognosis is comparably more favorable than that of conventional MPNST, though recurrence and distant metastases are not uncommon [120].

## Molecular Diagnostic Features

Karyotypic analyses [122–124], and more recently array comparative genomic hybridization (CGH) [103, 125] of MPNSTs have indicated that the vast majority of these tumors harbor structural and numerical chromosomal aberrations. Balanced translocations are rare [124], whereas microsatellite instability may be detected in up to one third of cases [122]. The majority of MPNSTs (including both sporadic and NF1-associated) have gross inactivating alterations of the p16 (INK4A) gene on 9p21 [126–128]; though inactivation is mainly via deletions and rearrangements [128], promoter methylation may also play a role [127]. EGFR [129, 130], topoisomerase-IIα [131], neuregulin-1/erbB and insulin-like growth factor 1 receptor pathways [132, 133] have all been implicated in MPNST tumorigenesis, as have microRNAs mirR-204 and miR-21 [134, 135]. Gene expression profiling studies have indicated distinct molecular classes of MPNST, and have found overexpression of neural stem cell markers sox9 and TWIST1, and neuroglial differentiation-associated transcripts; these finding may be important for future targeted therapies [136–138].

## Differential Diagnosis

Unfortunately, there are no specific histologic characteristics that allow for reliable differentiation of MPNST from other malignant sarcomas. Demonstration of origination from a peripheral nerve or underlying neurofibroma is clearly helpful, though is not always present. The fallback is therefore immunohistochemistry, which is used to help provide evidence of nerve sheath differentiation in MPNST and at the same time rule out other tumor types. Ultrastructural examination may be helpful in some cases, in demonstrating intratumoral basement membrane material, or the sarcomeric structures of MTT [114].

Differentiation of MPNST from monophasic synovial sarcoma (SS) can be particularly problematic as the later may involve nerves on occasion, and can express S100; MPNST can likewise rarely express EMA and low molecular weight cytokeratin [40, 93, 114]. Findings of cellular pleomorphism and CD34 positive cells would favor MPNST [40, 93] over SS. Sox10, if positive, may be useful as it represents a more reliable marker of neural crest origin then S100, and is typically negative in non-neural sarcoma which might otherwise be confused with MPNST [97]. TLE1 is a transcriptional corepressor overexpressed in synovial sarcoma; diffuse nuclear staining with anti-TLE1 antibody is seen in SS, whereas MPNST is typically negative [139]. Determination of SYT status by immunohistochemistry may be similarly helpful [140], being consistently positive in SS, paralleling the expected SYT-associated translocations demonstrable by FISH [141] or other molecular modalities; SYT alterations, in contradistinction, are not expected in MPNSTs. Leiomyosarcoma and solitary fibrous tumor are two other mimics; happily, immunopositivity for smooth muscle actin (SMA) and diffuse CD34 positivity, respectively, reliably separate these spindle cell neoplasms from MPNST.

Certain variant MPNSTs deserve specific comment with regard to differential diagnosis. For instance, PNET-like areas may be present, sometimes extensively, with MPNST (Fig. 15.16). Though these foci are immunopositive for NCAM and synaptophysin, their absence of CD99 staining and/or EWS-related translocations reliably distinguishes them from peripheral PNET/Ewing sarcoma [106]. Epithelioid MPNST may closely resemble melanoma, clear cell and epithelioid sarcoma, or carcinoma. Absence of melanoma markers (HMB45 or MART1) effectively distinguishes the former from both malignant melanoma and clear cell sarcoma, while the lack of cytokeratin positivity and presence of diffuse positivity for S100 excludes both carcinoma and epithelioid sarcoma [40, 93].

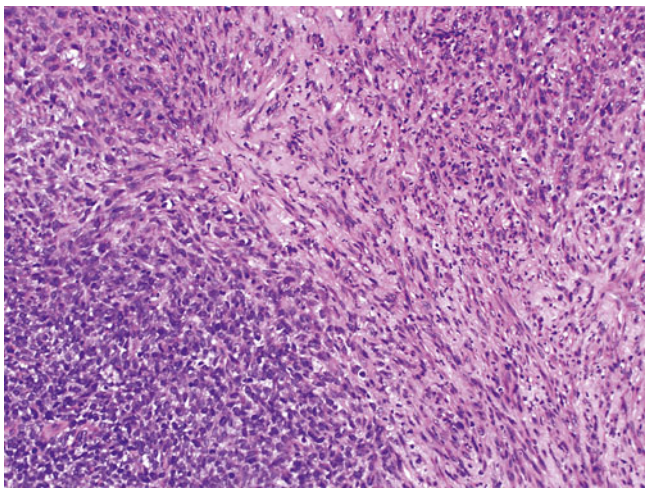

**Fig. 15.16** MPNST with PNET-like focus, comprising closely packed sheets of Ewing sarcoma-like small blue cells that segue into a central spindle cell zone

Once considered a variant of MPNST, plexiform cellular schwannoma (PCS) has no metastatic potential though does tend to recur locally. It is frequently congenital, presenting in infants, and is unassociated with NF1. Grossly PCS is multinodular or plexiform in configuration with a homogeneous interior; the histology correlate is a hypercellular spindle cell lesion composed of cells with elongated hyperchromatic nuclei, indistinct cell boards, and variable mitotic/proliferative activity. Unlike classic MPNST, PCS is composed solely of neoplastic Schwann cells, displaying uniform S100 expression; nuclear p53 accumulation is likewise lacking in the later [142].

## Treatment and Prognostic Features

MPNSTs are locally aggressive sarcomas with an added propensity to metastasize throughout the body. About half will show local recurrence, and 40 % will show multifocality and/or metastasis [2]. The overall survival rate is approximately 50 % at 3 years and 43 % at 5 years [143]. Delay in diagnosis is not uncommon, especially for tumors arising in more proximal or head/neck locations. Consistent predictors of worse patient prognosis include young patient age (<30 years) [2, 48], large size (>5 cm) [143–145], high tumor grade and stage [2, 5, 143, 144]. MPNSTs arising from the dura or within the neck or torso, and MTT in general, appear to be particularly aggressive [5, 13, 16, 112, 113, 146, 147]. MPNSTs arising within the context of NF1 tend to occur in younger patients and be associated with a significantly shorter progression-free survival [5, 112, 148]. Irrespective of patient NF1 status, complete surgical resection with adequate margins is the principal goal of treatment for MPNST [3, 148, 149]. Adjuvant radiation therapy offers improved survival, whereas the role of chemotherapy is more questionable [148, 149]. Of interest, histone deacetylase inhibitors (HDACi) have shown some promise in treating a subset of NF1-associated MPNSTs, but this efficacy is not seen in sporadic MPNSTs [150].

A number of molecular alterations detectable in MPNST may provide important prognostic clues and/or potential therapeutic targets. Overexpressions of EGFR, IGF1R, topoIIα, FOXM1, and p53 have all been implicated as indicators of poor patient survival [102, 130, 131, 133, 151]. Inactivation of p14 (ARF) and p16 (INK4a) have also been associated with poor prognosis in MPNSTs [152]. Independent studies have found PDGFRA, PDGFRB, EGFR, mTOR, and the PI3K/AKT pathways as promising targets for novel therapies [153, 154]. Tamoxifen has been shown to inhibit MPNST cell proliferation and survival [155], and combination therapies using ErbB2 with EGFR inhibitors or agents inducing lysosomal dysfunction have shown promise as well [129, 156, 157].

## References


1. Perrin RG, Guha A. Malignant peripheral nerve sheath tumors. Neurosurg Clin N Am. 2004;15:203–16.
2. Rekhi B, Ingle A, Kumar R, et al. Malignant peripheral nerve sheath tumors: clinicopathological profile of 63 cases diagnosed at a tertiary cancer referral center in Mumbai, India. Ind J Pathol Microbiol. 2010;53:611–8.
3. Dunn GP, Spiliopoulos K, Plotkin SR, et al. Role of resection of malignant peripheral nerve sheath tumors in patients with neurofibromatosis type 1. J Neurosurg. 2013;118:142–8.
4. Tucker T, Wolkenstein P, Revuz J, et al. Association between benign and malignant peripheral nerve sheath tumors in NF1. Neurology. 2005;65:205–11.
5. Stucky CC, Johnson KN, Gray RJ, et al. Malignant peripheral nerve sheath tumors (MPNST): the Mayo Clinic experience. Ann Surg Oncol. 2012;19:878–85.
6. Hagel C, Zils U, Peiper M, et al. Histopathology and clinical outcome of NF1-associated vs. sporadic malignant peripheral nerve sheath tumors. J Neurooncol. 2007;82:187–92.
7. Adamson DC, Cummings TJ, Friedman AH. Malignant peripheral nerve sheath tumor of the spine after radiation therapy for Hodgkin's lymphoma. Clin Neuropathol. 2004;23:245–55.
8. Amin A, Saifuddin A, Flanagan A, et al. Radiotherapy-induced malignant peripheral nerve sheath tumor of the cauda equina. Spine. 2004;29:E506–9.
9. Albayrak BS, Gorgulu A, Kose T. A case of intra-dural malignant peripheral nerve sheath tumor in thoracic spine associated with neurofibromatosis type 1. J Neurooncol. 2006;78:187–90.
10. Imazu M, Nakamura Y, Nakatani H, et al. Cervicothoracic malignant peripheral nerve sheath tumor in a 12-year-old girl with neurofibromatosis type 1. Eur J Pediatr Surg. 2006;16:285–7.
11. Chamoun RB, Whitehead WE, Dauser RC, et al. Primary disseminated intradural malignant peripheral nerve sheath tumor of the spine in a child: case report and review of the literature. Pediatr Neurosurg. 2009;45:230–6.
12. Yone K, Ijiri K, Hayashi K, et al. Primary malignant peripheral nerve sheath tumor of the cauda equina in a child case report. Spinal Cord. 2004;42:199–203.
13. Xu Q, Xing B, Huang X, et al. Primary malignant peripheral nerve sheath tumor of the cauda equina with metastasis to the brain in a child: case report and literature review. Spine J. 2012;12:e7–13.
14. Mut M, Cataltepe O, Soylemezoglu F, et al. Radiation-induced malignant triton tumor associated with severe spinal cord compression. Case report and review of the literature. J Neurosurg. 2004;100:298–302.
15. James G, Crocker M, King A, et al. Malignant triton tumors of the spine. J Neurosurg Spine. 2008;8:567–73.
16. Prieto R, Pascual JM, Garcia-Cabezas MA, et al. Low-grade malignant triton tumor in the lumbar spine: a rare variant of malignant peripheral nerve sheath tumor with rhabdomyoblastic differentiation. Neuropathology. 2012;32:180–9.
17. Ghosh A, Sastri SB, Srinivas D, et al. Malignant triton tumor of cervical spine with hemorrhage. J Clin Neurosci. 2011;18:721–3.
18. Scheithauer BW, Erdogan S, Rodriguez FJ, et al. Malignant peripheral nerve sheath tumors of cranial nerves and intracranial contents: a clinicopathologic study of 17 cases. Am J Surg Pathol. 2009;33:325–38.
19. Ziadi A, Saliba I. Malignant peripheral nerve sheath tumor of intracranial nerve: a case series review. Auris Nasus Larynx. 2010;37:539–45.
20. Ueda R, Saito R, Horiguchi T, et al. Malignant peripheral nerve sheath tumor in the anterior skull base associated with neurofibromatosis type 1–case report. Neurol Med Chir (Tokyo). 2004;44:38–42.

21. Rawal A, Yin Q, Roebuck M, et al. Atypical and malignant peripheral nerve-sheath tumors of the brachial plexus: report of three cases and review of the literature. Microsurgery. 2006;26:80–6.
22. Garg A, Gupta V, Gaikwad SB, et al. Scalp malignant peripheral nerve sheath tumor (MPNST) with bony involvement and new bone formation: case report. Clin Neurol Neurosurg. 2004;106:340–4.
23. Ge P, Fu S, Lu L, et al. Diffuse scalp malignant peripheral nerve sheath tumor with intracranial extension in a patient with neurofibromatosis type 1. J Clin Neurosci. 2010;17:1443–4.
24. Minovi A, Basten O, Hunter B, et al. Malignant peripheral nerve sheath tumors of the head and neck: management of 10 cases and literature review. Head Neck. 2007;29:439–45.
25. Telera S, Carapella C, Covello R, et al. Malignant peripheral nerve sheath tumors of the lateral skull base. J Craniofac Surg. 2008; 19:805–12.
26. Sanchez-Mejia RO, Pham DN, Prados M, et al. Management of a sporadic malignant subfrontal peripheral nerve sheath tumor. J Neurooncol. 2006;76:165–9.
27. Ahsan F, Lee MK, Ah-See KW, et al. Malignant peripheral nerve sheath tumor of the paranasal sinuses. Ear Nose Throat J. 2004; 83:699–701.
28. Neetha MC, Anupama DH, Shashikanth MC. Malignant peripheral nerve sheath tumor of the maxilla. Indian J Dent Res. 2004;15:110–3.
29. Zakhary I, Elsalanty M, Ishag I, et al. Malignant peripheral nerve sheath tumor of mandible. J Craniofac Surg. 2011;22:762–6.
30. Nepka C, Karadana M, Karasavvidou F, et al. Fine needle aspiration cytology of a primary malignant peripheral nerve sheath tumor arising in the parotid gland: a case report. Acta Cytol. 2009;53:423–6.
31. Imamura S, Suzuki H, Koda E, et al. Malignant peripheral nerve sheath tumor of the parotid gland. Ann Otol Rhinol Laryngol. 2003;112:637–43.
32. Aslan I, Oysu C, Bilgic B, et al. Malignant peripheral nerve sheath tumor of the parotid gland. Kulak Burun Bogaz Ihtis Derg. 2007;17:53–7.
33. Allison KH, Patel RM, Goldblum JR, et al. Superficial malignant peripheral nerve sheath tumor: a rare and challenging diagnosis. Am J Clin Pathol. 2005;124:685–92.
34. Thomas C, Somani N, Owen LG, et al. Cutaneous malignant peripheral nerve sheath tumors. J Cutan Pathol. 2009;36:896–900.
35. Al Akloby O, Bukhari IA, El-Shawarby M, et al. Malignant peripheral nerve sheath tumor of the skin: case report. Am J Clin Dermatol. 2006;7:201–3.
36. Kabir S, Kapetanakis EI, Shabbo F. Intracardiac malignant Triton tumor: a first presentation. Ann Thorac Surg. 2010;89:968–9.
37. Kobori L, Nagy P, Mathe Z, et al. Malignant peripheral nerve sheath tumor of the liver: a case report. Pathol Oncol Res. 2008; 14:329–32.
38. Matsuo K, Nagano Y, Sugimori K, et al. Primary malignant peripheral nerve-sheath tumor of the common bile duct. J Gastroenterol. 2005;40:306–11.
39. Lee YJ, Moon H, Park ST, et al. Malignant peripheral nerve sheath tumor arising from the colon in a newborn: report of a case and review of the literatures. J Pediatr Surg. 2006;41:e19–22.
40. Rodriguez AO, Truskinovsky AM, Kasrazadeh M, et al. Case report: malignant peripheral nerve sheath tumor of the uterine cervix treated with radical vaginal trachelectomy. Gynecol Oncol. 2006;100:201–4.
41. De A Focchi GR, Cuatrecasas M, Prat J. Malignant peripheral nerve sheath tumor of the uterine corpus: a case report. Int J Gynecol Pathol. 2007;26:437–40.
42. Gulati N, Rekhi B, Suryavanshi P, et al. Epithelioid malignant peripheral nerve sheath tumor of the uterine corpus. Ann Diagn Pathol. 2011;15:441–5.
43. Thanapaisal C, Koonmee S, Siritunyaporn S. Malignant peripheral nerve sheath tumor of breast in patient without Von Recklinghausen's neurofibromatosis: a case report. J Med Assoc Thai. 2006;89:377–9.
44. Dhingra KK, Mandal S, Roy S, et al. Malignant peripheral nerve sheath tumor of the breast: case report. World J Surg Oncol. 2007; 5:142.
45. Jankulovski N, Stankov O, Banev S, et al. Isolated malignant peripheral nerve sheath tumor of kidney capsule. Prilozi. 2008; 29:361–9.
46. Moon SJ, Lee JK, Seo BR, et al. An intraosseous malignant peripheral nerve sheath tumor of the cervical spine: a case report and review of the literature. Spine. 2008;33:E712–6.
47. de Chadarevian JP, MaePascasio J, Halligan GE, et al. Malignant peripheral nerve sheath tumor arising from an adrenal ganglioneuroma in a 6-year-old boy. Pediatr Dev Pathol. 2004;7:277–84.
48. Rekhi B, Jambhekar NA. Malignant transformation in a hybrid schwannoma/perineurioma: addition to the spectrum of a malignant peripheral nerve sheath tumor. Indian J Pathol Microbiol. 2011;54:825–8.
49. Pilavaki M, Chourmouzi D, Kiziridou A, et al. Imaging of peripheral nerve sheath tumors with pathologic correlation: pictorial review. Eur J Radiol. 2004;52:229–39.
50. Abreu E, Aubert S, Wavreille G, et al. Peripheral tumor and tumor-like neurogenic lesions. Eur J Radiol. 2013;82:38–50.
51. Hassell DS, Bancroft LW, Kransdorf MJ, et al. Imaging appearance of diffuse neurofibroma. AJR Am J Roentgenol. 2008;190:582–8.
52. Kele H. Ultrasonography of the peripheral nervous system. Perspect Med. 2012;1:417–21.
53. Reynolds Jr DL, Jacobson JA, Inampudi P, et al. Sonographic characteristics of peripheral nerve sheath tumors. AJR Am J Roentgenol. 2004;182:741–4.
54. Chen W, Jia JW, Wang JR. Soft tissue diffuse neurofibromas: sonographic findings. J Ultrasound Med. 2007;26:513–8.
55. Tsai WC, Chiou HJ, Chou YH, et al. Differentiation between schwannomas and neurofibromas in the extremities and superficial body: the role of high-resolution and color Doppler ultrasonography. J Ultrasound Med. 2008;27:161–6. quiz 168-169.
56. Hrehorovich PA, Franke HR, Maximin S, et al. Malignant peripheral nerve sheath tumor. Radiographics. 2003;23:790–4.
57. Murovic JA, Kim DH, Kline DG. Neurofibromatosis-associated nerve sheath tumors. Case report and review of the literature. Neurosurg Focus. 2006;20:E1.
58. Li CS, Huang GS, Wu HD, et al. Differentiation of soft tissue benign and malignant peripheral nerve sheath tumors with magnetic resonance imaging. Clin Imaging. 2008;32:121–7.
59. Banks KP. The target sign: extremity. Radiology. 2005;234:899–900.
60. Singh T, Kliot M. Imaging of peripheral nerve tumors. Neurosurg Focus. 2007;22:E6.
61. Woertler K. Tumors and tumor-like lesions of peripheral nerves. Semin Musculoskelet Radiol. 2010;14:547–58.
62. Bhargava R, Parham DM, Lasater OE, et al. MR imaging differentiation of benign and malignant peripheral nerve sheath tumors: use of the target sign. Pediatr Radiol. 1997;27:124–9.
63. Laffan EE, Ngan BY, Navarro OM. Pediatric soft-tissue tumors and pseudotumors: MR imaging features with pathologic correlation: part 2. Tumors of fibroblastic/myofibroblastic, so-called fibrohistiocytic, muscular, lymphomatous, neurogenic, hair matrix, and uncertain origin. Radiographics. 2009;29:e36.
64. O'Keefe P, Reid J, Morrison S, et al. Unexpected diagnosis of superficial neurofibroma in a lesion with imaging features of a vascular malformation. Pediatr Radiol. 2005;35:1250–3.
65. Lim R, Jaramillo D, Poussaint TY, et al. Superficial neurofibroma: a lesion with unique MRI characteristics in patients with neurofibromatosis type 1. AJR Am J Roentgenol. 2005;184:962–8.
66. Rha SE, Byun JY, Jung SE, et al. Neurogenic tumors in the abdomen: tumor types and imaging characteristics. Radiographics. 2003;23:29–43.

67. Lin J, Martel W. Cross-sectional imaging of peripheral nerve sheath tumors: characteristic signs on CT, MR imaging, and sonography. AJR Am J Roentgenol. 2001;176:75–82.
68. Beaman FD, Kransdorf MJ, Menke DM. Schwannoma: radiologic-pathologic correlation. Radiographics. 2004;24:1477–81.
69. Nilsson J, Sandberg K, Soe Nielsen N, et al. Magnetic resonance imaging of peripheral nerve tumours in the upper extremity. Scand J Plast Reconstr Surg Hand Surg. 2009;43:153–9.
70. Cerofolini E, Landi A, DeSantis G, et al. MR of benign peripheral nerve sheath tumors. J Comput Assist Tomogr. 1991;15:593–7.
71. Murphey MD, Smith WS, Smith SE, et al. From the archives of the AFIP. Imaging of musculoskeletal neurogenic tumors: radiologic-pathologic correlation. Radiographics. 1999;19:1253–80.
72. Gupta G, Maniker A. Malignant peripheral nerve sheath tumors. Neurosurg Focus. 2007;22:E12.
73. King AA, Debaun MR, Riccardi VM, et al. Malignant peripheral nerve sheath tumors in neurofibromatosis 1. Am J Med Genet. 2000;93:388–92.
74. Stull MA, Moser Jr RP, Kransdorf MJ, et al. Magnetic resonance appearance of peripheral nerve sheath tumors. Skeletal Radiol. 1991;20:9–14.
75. Demir HA, Varan A, Yalcn B, et al. Malignant peripheral nerve sheath tumors in childhood: 13 cases from a single center. J Pediatr Hematol Oncol. 2012;34:204–7.
76. Ferner RE, Gutmann DH. International consensus statement on malignant peripheral nerve sheath tumors in neurofibromatosis. Cancer Res. 2002;62:1573–7.
77. Gruber H, Glodny B, Bendix N, et al. High-resolution ultrasound of peripheral neurogenic tumors. Eur Radiol. 2007;17:2880–8.
78. Levine E, Huntrakoon M, Wetzel LH. Malignant nerve-sheath neoplasms in neurofibromatosis: distinction from benign tumors by using imaging techniques. AJR Am J Roentgenol. 1987;149: 1059–64.
79. Nguyen R, Dombi E, Widemann BC, et al. Growth dynamics of plexiform neurofibromas: a retrospective cohort study of 201 patients with neurofibromatosis 1. Orphanet J Rare Dis. 2012;7:75.
80. Dombi E, Solomon J, Gillespie AJ, et al. NF1 plexiform neurofibroma growth rate by volumetric MRI: relationship to age and body weight. Neurology. 2007;68:643–7.
81. Ferner RE, Huson SM, Thomas N, et al. Guidelines for the diagnosis and management of individuals with neurofibromatosis 1. J Med Genet. 2007;44:81–8.
82. Tucker T, Friedman JM, Friedrich RE, et al. Longitudinal study of neurofibromatosis 1 associated plexiform neurofibromas. J Med Genet. 2009;46:81–5.
83. Wasa J, Nishida Y, Tsukushi S, et al. MRI features in the differentiation of malignant peripheral nerve sheath tumors and neurofibromas. AJR Am J Roentgenol. 2010;194:1568–74.
84. Mautner VF, Asuagbor FA, Dombi E, et al. Assessment of benign tumor burden by whole-body MRI in patients with neurofibromatosis 1. Neuro Oncol. 2008;10:593–8.
85. Brenner W, Friedrich RE, Gawad KA, et al. Prognostic relevance of FDG PET in patients with neurofibromatosis type-1 and malignant peripheral nerve sheath tumours. Eur J Nucl Med Mol Imaging. 2006;33:428–32.
86. Bredella MA, Torriani M, Hornicek F, et al. Value of PET in the assessment of patients with neurofibromatosis type 1. AJR Am J Roentgenol. 2007;189:928–35.
87. Ferner RE, Golding JF, Smith M, et al. [18 F]2-fluoro-2-deoxy-D-glucose positron emission tomography (FDG PET) as a diagnostic tool for neurofibromatosis 1 (NF1) associated malignant peripheral nerve sheath tumours (MPNSTs): a long-term clinical study. Ann Oncol. 2008;19:390–4.
88. Son JM, Ahn MI, Cho KD, et al. Varying degrees of FDG uptake in multiple benign neurofibromas on PET/CT. Br J Radiol. 2007;80:e222–6.
89. Warbey VS, Ferner RE, Dunn JT, et al. [18 F]FDG PET/CT in the diagnosis of malignant peripheral nerve sheath tumours in neurofibromatosis type-1. Eur J Nucl Med Mol Imaging. 2009;36: 751–7.
90. Benz MR, Czernin J, Dry SM, et al. Quantitative F18-fluorodeoxyglucose positron emission tomography accurately characterizes peripheral nerve sheath tumors as malignant or benign. Cancer. 2010;116:451–8.
91. Tsai LL, Drubach L, Fahey F, et al. [18 F]-Fluorodeoxyglucose positron emission tomography in children with neurofibromatosis type 1 and plexiform neurofibromas: correlation with malignant transformation. J Neurooncol. 2012;108:469–75.
92. Meany H, Dombi E, Reynolds J, et al. 18-fluorodeoxyglucose-positron emission tomography (FDG-PET) evaluation of nodular lesions in patients with Neurofibromatosis type 1 and plexiform neurofibromas (PN) or malignant peripheral nerve sheath tumors (MPNST). Pediatr Blood Cancer. 2013;60:59–64.
93. Rodriguez FJ, Scheithauer BW, Abell-Aleff PC, et al. Low grade malignant peripheral nerve sheath tumor with smooth muscle differentiation. Acta Neuropathol. 2007;113:705–9.
94. Wakely Jr PE, Ali SZ, Bishop JA. The cytopathology of malignant peripheral nerve sheath tumor: a report of 55 fine-needle aspiration cases. Cancer Cytopathol. 2012;120:334–41.
95. Gupta K, Dey P, Vashisht R. Fine-needle aspiration cytology of malignant peripheral nerve sheath tumors. Diagn Cytopathol. 2004;31:1–4.
96. Olsen SH, Thomas DG, Lucas DR. Cluster analysis of immunohistochemical profiles in synovial sarcoma, malignant peripheral nerve sheath tumor, and Ewing sarcoma. Mod Pathol. 2006;19: 659–68.
97. Karamchandani JR, Nielsen TO, van de Rijn M, et al. Sox10 and S100 in the diagnosis of soft-tissue neoplasms. Appl Immunohistochem Mol Morphol. 2012;20:445–50.
98. Zhou H, Coffin CM, Perkins SL, et al. Malignant peripheral nerve sheath tumor: a comparison of grade, immunophenotype, and cell cycle/growth activation marker expression in sporadic and neurofibromatosis 1-related lesions. Am J Surg Pathol. 2003;27:1337–45.
99. Hirose T, Tani T, Shimada T, et al. Immunohistochemical demonstration of EMA/Glut1-positive perineurial cells and CD34-positive fibroblastic cells in peripheral nerve sheath tumors. Mod Pathol. 2003;16:293–8.
100. Nonaka D, Chiriboga L, Rubin BP. Sox10: a pan-schwannian and melanocytic marker. Am J Surg Pathol. 2008;32:1291–8.
101. Giangaspero F, Fratamico FC, Ceccarelli C, et al. Malignant peripheral nerve sheath tumors and spindle cell sarcomas: an immunohistochemical analysis of multiple markers. Appl Pathol. 1989;7:134–44.
102. Brekke HR, Kolberg M, Skotheim RI, et al. Identification of p53 as a strong predictor of survival for patients with malignant peripheral nerve sheath tumors. Neuro Oncol. 2009;11:514–28.
103. Brekke HR, Ribeiro FR, Kolberg M, et al. Genomic changes in chromosomes 10, 16, and X in malignant peripheral nerve sheath tumors identify a high-risk patient group. J Clin Oncol. 2010;28:1573–82.
104. Ducatman BS, Scheithauer BW. Malignant peripheral nerve sheath tumors with divergent differentiation. Cancer. 1984;54: 1049–57.
105. Han JC, Kim YD, Suh YL, et al. Fibroblastic low-grade malignant peripheral nerve sheath tumor in the orbit. Ophthal Plast Reconstr Surg. 2012;28:e97–8.
106. Shintaku M, Nakade M, Hirose T. Malignant peripheral nerve sheath tumor of small round cell type with pleomorphic spindle cell sarcomatous areas. Pathol Int. 2003;53:478–82.
107. Suresh TN, Harendra Kumar ML, Prasad CS, et al. Malignant peripheral nerve sheath tumor with divergent differentiation. Indian J Pathol Microbiol. 2009;52:74–6.

108. Huang L, Espinoza C, Welsh R. Malignant peripheral nerve sheath tumor with divergent differentiation. Arch Pathol Lab Med. 2003; 127:e147–50.
109. Tirabosco R, Galloway M, Bradford R, et al. Liposarcomatous differentiation in malignant peripheral nerve sheath tumor: a case report. Pathol Res Pract. 2010;206:138–42.
110. Ballas K, Kontoulis TM, Papavasiliou A, et al. A rare case of malignant triton tumor with pluridirectional differentiation. South Med J. 2009;102:435–7.
111. Janczar K, Tybor K, Jozefowicz M, et al. Low grade malignant peripheral nerve sheath tumor with mesenchymal differentiation: a case report. Pol J Pathol. 2011;62:278–81.
112. Kamran SC, Howard SA, Shinagare AB, et al. Malignant peripheral nerve sheath tumors: prognostic impact of rhabdomyoblastic differentiation (malignant triton tumors), neurofibromatosis 1 status and location. Eur J Surg Oncol. 2013;39:46–52.
113. Brooks JS, Freeman M, Enterline HT. Malignant "Triton" tumors. Natural history and immunohistochemistry of nine new cases with literature review. Cancer. 1985;55:2543–9.
114. Stasik CJ, Tawfik O. Malignant peripheral nerve sheath tumor with rhabdomyosarcomatous differentiation (malignant triton tumor). Arch Pathol Lab Med. 2006;130:1878–81.
115. Lodding P, Kindblom LG, Angervall L. Epithelioid malignant schwannoma. A study of 14 cases. Virchows Arch A Pathol Anat Histopathol. 1986;409:433–51.
116. Laskin WB, Weiss SW, Bratthauer GL. Epithelioid variant of malignant peripheral nerve sheath tumor (malignant epithelioid schwannoma). Am J Surg Pathol. 1991;15:1136–45.
117. Prescott DK, Racz MM, Ng JD. Epithelioid malignant peripheral nerve sheath tumor in the infraorbital nerve. Ophthal Plast Reconstr Surg. 2006;22:150–1.
118. Carter JM, O'Hara C, Dundas G, et al. Epithelioid malignant peripheral nerve sheath tumor arising in a schwannoma, in a patient with "neuroblastoma-like" schwannomatosis and a novel germline SMARCB1 mutation. Am J Surg Pathol. 2012;36:154–60.
119. Woodruff JM, Christensen WN. Glandular peripheral nerve sheath tumors. Cancer. 1993;72:3618–28.
120. Hirose T, Scheithauer BW, Sano T. Perineurial malignant peripheral nerve sheath tumor (MPNST): a clinicopathologic, immunohistochemical, and ultrastructural study of seven cases. Am J Surg Pathol. 1998;22:1368–78.
121. Mitchell A, Scheithauer BW, Doyon J, et al. Malignant perineurioma (malignant peripheral nerve sheath tumor with perineural differentiation). Clin Neuropathol. 2012;31:424–9.
122. Kobayashi C, Oda Y, Takahira T, et al. Chromosomal aberrations and microsatellite instability of malignant peripheral nerve sheath tumors: a study of 10 tumors from nine patients. Cancer Genet Cytogenet. 2006;165:98–105.
123. Haddadin MH, Hawkins AL, Long P, et al. Cytogenetic study of malignant triton tumor: a case report. Cancer Genet Cytogenet. 2003;144:100–5.
124. Gil Z, Fliss DM, Voskoboimik N, et al. Two novel translocations, t(2;4)(q35;q31) and t(X;12)(q22;q24), as the only karyotypic abnormalities in a malignant peripheral nerve sheath tumor of the skull base. Cancer Genet Cytogenet. 2003;145:139–43.
125. Mantripragada KK, Diaz de Stahl T, Patridge C, et al. Genome-wide high-resolution analysis of DNA copy number alterations in NF1-associated malignant peripheral nerve sheath tumors using 32K BAC array. Genes Chromosomes Cancer. 2009;48:897–907.
126. Sabah M, Cummins R, Leader M, et al. Loss of p16 (INK4A) expression is associated with allelic imbalance/loss of heterozygosity of chromosome 9p21 in microdissected malignant peripheral nerve sheath tumors. Appl Immunohistochem Mol Morphol. 2006;14:97–102.
127. Perrone F, Tabano S, Colombo F, et al. p15INK4b, p14ARF, and p16INK4a inactivation in sporadic and neurofibromatosis type 1-related malignant peripheral nerve sheath tumors. Clin Cancer Res. 2003;9:4132–8.
128. Agesen TH, Florenes VA, Molenaar WM, et al. Expression patterns of cell cycle components in sporadic and neurofibromatosis type 1-related malignant peripheral nerve sheath tumors. J Neuropathol Exp Neurol. 2005;64:74–81.
129. Holtkamp N, Malzer E, Zietsch J, et al. EGFR and erbB2 in malignant peripheral nerve sheath tumors and implications for targeted therapy. Neuro Oncol. 2008;10:946–57.
130. Keizman D, Issakov J, Meller I, et al. Expression and significance of EGFR in malignant peripheral nerve sheath tumor. J Neurooncol. 2009;94:383–8.
131. Skotheim RI, Kallioniemi A, Bjerkhagen B, et al. Topoisomerase-II alpha is upregulated in malignant peripheral nerve sheath tumors and associated with clinical outcome. J Clin Oncol. 2003;21:4586–91.
132. Stonecypher MS, Byer SJ, Grizzle WE, et al. Activation of the neuregulin-1/ErbB signaling pathway promotes the proliferation of neoplastic Schwann cells in human malignant peripheral nerve sheath tumors. Oncogene. 2005;24:5589–605.
133. Yang J, Ylipaa A, Sun Y, et al. Genomic and molecular characterization of malignant peripheral nerve sheath tumor identifies the IGF1R pathway as a primary target for treatment. Clin Cancer Res. 2011;17:7563–73.
134. Gong M, Ma J, Li M, et al. MicroRNA-204 critically regulates carcinogenesis in malignant peripheral nerve sheath tumors. Neuro Oncol. 2012;14:1007–17.
135. Itani S, Kunisada T, Morimoto Y, et al. MicroRNA-21 correlates with tumorigenesis in malignant peripheral nerve sheath tumor (MPNST) via programmed cell death protein 4 (PDCD4). J Cancer Res Clin Oncol. 2012;138:1501–9.
136. Watson MA, Perry A, Tihan T, et al. Gene expression profiling reveals unique molecular subtypes of Neurofibromatosis Type I-associated and sporadic malignant peripheral nerve sheath tumors. Brain Pathol. 2004;14:297–303.
137. Miller SJ, Rangwala F, Williams J, et al. Large-scale molecular comparison of human Schwann cells to malignant peripheral nerve sheath tumor cell lines and tissues. Cancer Res. 2006;66:2584–91.
138. Holtkamp N, Mautner VF, Friedrich RE, et al. Differentially expressed genes in neurofibromatosis 1-associated neurofibromas and malignant peripheral nerve sheath tumors. Acta Neuropathol. 2004;107:159–68.
139. Jagdis A, Rubin BP, Tubbs RR, et al. Prospective evaluation of TLE1 as a diagnostic immunohistochemical marker in synovial sarcoma. Am J Surg Pathol. 2009;33:1743–51.
140. He R, Patel RM, Alkan S, et al. Immunostaining for SYT protein discriminates synovial sarcoma from other soft tissue tumors: analysis of 146 cases. Mod Pathol. 2007;20:522–8.
141. Tanas MR, Rubin BP, Tubbs RR, et al. Utilization of fluorescence in situ hybridization in the diagnosis of 230 mesenchymal neoplasms: an institutional experience. Arch Pathol Lab Med. 2010;134:1797–803.
142. Woodruff JM, Scheithauer BW, Kurtkaya-Yapicier O, et al. Congenital and childhood plexiform (multinodular) cellular schwannoma: a troublesome mimic of malignant peripheral nerve sheath tumor. Am J Surg Pathol. 2003;27:1321–9.
143. Okada K, Hasegawa T, Tajino T, et al. Clinical relevance of pathological grades of malignant peripheral nerve sheath tumor: a multi-institution TMTS study of 56 cases in Northern Japan. Ann Surg Oncol. 2007;14:597–604.
144. Zou C, Smith KD, Liu J, et al. Clinical, pathological, and molecular variables predictive of malignant peripheral nerve sheath tumor outcome. Ann Surg. 2009;249:1014–22.
145. Baehring JM, Betensky RA, Batchelor TT. Malignant peripheral nerve sheath tumor: the clinical spectrum and outcome of treatment. Neurology. 2003;61:696–8.
146. Terzic A, Bode B, Gratz KW, et al. Prognostic factors for the malignant triton tumor of the head and neck. Head Neck. 2009;31:679–88.

147. McConnell YJ, Giacomantonio CA. Malignant triton tumors–complete surgical resection and adjuvant radiotherapy associated with improved survival. J Surg Oncol. 2012;106:51–6.
148. Moretti VM, Crawford EA, Staddon AP, et al. Early outcomes for malignant peripheral nerve sheath tumor treated with chemotherapy. Am J Clin Oncol. 2011;34:417–21.
149. Gachiani J, Kim D, Nelson A, et al. Surgical management of malignant peripheral nerve sheath tumors. Neurosurg Focus. 2007;22:E13.
150. Lopez G, Torres K, Liu J, et al. Autophagic survival in resistance to histone deacetylase inhibitors: novel strategies to treat malignant peripheral nerve sheath tumors. Cancer Res. 2011;71:185–96.
151. Yu J, Deshmukh H, Payton JE, et al. Array-based comparative genomic hybridization identifies CDK4 and FOXM1 alterations as independent predictors of survival in malignant peripheral nerve sheath tumor. Clin Cancer Res. 2011;17:1924–34.
152. Endo M, Kobayashi C, Setsu, N, et al. Prognostic significance of $p14^{ARF}$, $p15^{INK4b}$, and $p16^{INK4a}$ inactivation in malignant peripheral nerve sheath tumors. Clin Cancer Res. 2011;17:3771–82.
153. Zou CY, Smith KD, Zhu QS, et al. Dual targeting of AKT and mammalian target of rapamycin: a potential therapeutic approach for malignant peripheral nerve sheath tumor. Mol Cancer Ther. 2009;8:1157–68.
154. Perrone F, Da Riva L, Orsenigo M, et al. PDGFRA, PDGFRB, EGFR, and downstream signaling activation in malignant peripheral nerve sheath tumor. Neuro Oncol. 2009;11:725–36.
155. Byer SJ, Eckert JM, Brossier NM, et al. Tamoxifen inhibits malignant peripheral nerve sheath tumor growth in an estrogen receptor-independent manner. Neuro Oncol. 2011;13:28–41.
156. Dilworth JT, Wojtkowiak JW, Mathieu P, et al. Suppression of proliferation of two independent NF1 malignant peripheral nerve sheath tumor cell lines by the pan-ErbB inhibitor CI-1033. Cancer Biol Ther. 2008;7:1938–46.
157. Kohli L, Kaza N, Lavalley NJ, et al. The pan erbB inhibitor PD168393 enhances lysosomal dysfunction-induced apoptotic death in malignant peripheral nerve sheath tumor cells. Neuro Oncol. 2012;14:266–77.